The low-Ti basaltic rocks form a disrupted pile of pillowed extrusives with intercalated massive cooling units. Some of the latter are fine-grained intrusives (e.g. 005, 017; see Plate 5.6A) but others, especially the aphyric and vitrophyric types, might be massive flows (e.g. 019). Also in the type area of PBOC, a narrow (15-35 cm wide) amphibolitized low-Ti basaltic dyke (012) was found cutting partially amphibolitized cumulate gabbro. The nested- or sheeted-dyke sequences which underlie basaltic extrusives in many other ophiolitic assemblages (*cf.* Coleman, 1977) are not found in the PBOC. It is not known whether it is an intrinsic feature of the Complex or a function of structural controls. Thus, although the low-Ti basaltic pile is considerably disrupted by internal faulting, most of the units appear to have relatively shallow dips (see below) and consequently underlying feeder dykes might be as yet unexposed.

Pillowed extrusives constitute approximately 60-70% of the known outcrop of low-Ti basaltic rocks in the PBOC. Pillow morphologies are highly variable and range from small bulbous protrusions (<10 cm) to several metre long portions of lava tubes (Plate 5.6B,C,D,E). In cross-section the bulbous pillows and lava tubes usually display a hackly fracture pattern and the concentric and radial fractures more generally typical of pillow lavas (e.g. Wells *et al.*, 1979) are subordinate (e.g. Plate 5.6F). Cooling cracks are the only mesoscopic-scale structures evident in some low-Ti pillows but many display small-scale flow-banding (Plate 5.6G) and/or some radial variation in mesoscopic textural elements (see Section 5.7.2). Intra-pillow cavities are exceedingly rare, and vesicles are found only rarely in minor pillow breccias and in microdolerite at the top of the section.

Vesicles and carbonate- or chalcedony-filled amygdales in the pillow breccias generally range up to 3 mm or rarely up to 10 mm in longest dimension. They are only sparsely scattered throughout the pillow fragments and it is clear that brecciation was not directly related to vesiculation of the magmas. Unless these magmas were strongly oversaturated in CO_2, it is likely that they were extruded in relatively shallow water (<1 km, see Sections 3.6.1 and 5.7.2). At both localities these pillow breccias contain ferruginous veins (e.g. 015, 024), and jasper containing from 4%-10% Fe calculated as Fe_2O_3 (determined from microprobe scans) is a common interpillow filling (Plate 5.6H). Also, the pillow fragments are generally more chloritized than other low-Ti basaltic rocks in the area

PLATE 5.6

PBOC Low-Ti Basaltic Rocks, Tomalla Creek Section (Map 1)

A. Massive carbonate-veined microdolerite (left) intruding pillowed extrusives. White veins are carbonate.

B. Pillowed extrusive unit displaying portions of disrupted lava tubes (left). The underlying unit is apparently a massive extrusive (sub-variolitic texture). White veins in the latter are carbonate.

C-E. Pillow morphologies in PBOC low-Ti basaltic extrusives. The scales in C and D are slightly greater than half that in E. Darker, low-relief interpillow material is hyaloclastite (*cf.* Plate 5.7). Note budded pillows (C and D, centre), longitudinal sections through parts of lava tubes (C, centre left; D, upper centre), and large nested elongate pillows (? tubes; E).

F. Cross-section through an aphanitic lava tube which is largely surrounded by more massive lava. Note hackly mesoscopic texture and incipient development of radial cooling cracks. Other parts of the outcrop contain bulbous pillows. Some of the latter also appear to be isolated in relatively massive lava although, where present, interpillow material is more commonly hyaloclastite.

G. Small-scale flow-banding immediately beneath the outer rind (spalled off) of a relatively small lava tube (25 cm in diameter, scale 1:5, pen on upper margin is 1.5 cm in diameter).

H. Sparsely-developed interpillow hyaloclastite and interpillow jasper (e.g. dark rectangular and dark elongate cavity fillings, left of centre and lower left corner respectively) in vesicular/amygdaloidal pillow breccia. Pillows are relatively poorly-developed in the part of the outcrop illustrated. White veins are carbonate ± chalcedony.

PLATE 5·6

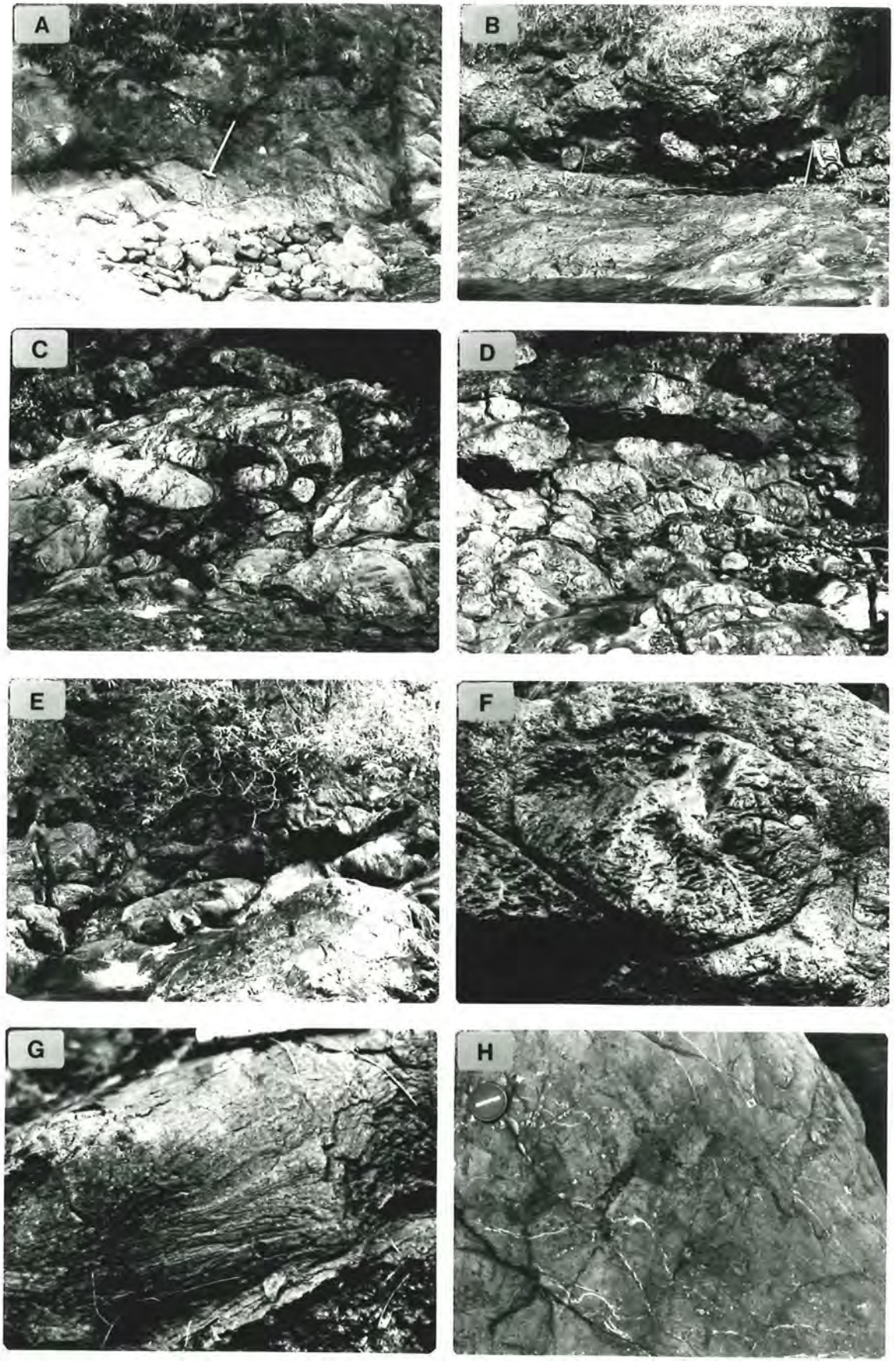

and it is likely that these breccias mark the former sites of minor submarine hydrothermal activity.

Most pillowed flows contain some interpillow hyaloclastite (Plate 5.6C,D), even where the pillows are relatively tightly packed (Plate 5.7A). Some flow units contain localized patches of dispersed pillow, or pillow-fragment breccia with abundant hyaloclastite matrix (Plate 5.7B). These are much smaller-scale features than the hyaloclastite stone streams developed on the unstable slopes of small seamounts (e.g. Lonsdale and Batiza, 1980) and typical interflow breccia or flow-foot talus deposits (*cf.* Ballard and Moore, 1977; Dimroth *et al.*, 1978). In most instances the PBOC hyaloclastite has accumulated in voids between irregularly-shaped pillows and these portions of the flows usually appear to consist of loosely-packed, randomly-oriented and occasionally budded lava tubes (Plates 5.6C,D and 5.7C,D ; *cf.* Moore, 1975; Ballard and Moore, 1977; Hargreaves and Ayres, 1979).

The hyaloclastite almost invariably consists of a closed to relatively dispersed framework of black angular fragments of chloritized non-vesicular sideromelane. These are set in white to cream or creamy green siliceous matrix (Plate 5.7E,F,G). The fragments range in size from sub-mesoscopic to ~10 cm and appear to have been derived solely from the shattered outer margins of the associated pillows (see Plate 5.7E). Fresh or partially chloritized fragments of variolitic (Plate 5.7F) or microlitic (Plate 5. G) low-Ti basalt are sparsely scattered throughout many of the coarser-grained hyaloclastite occurrences, but the vast majority of fragments have undergone pervasive hydrothermal alteration (see Section 5.7.2).

Almost all low-Ti basaltic outcrops contain abundant carbonate veins. These fill cooling fractures on all scales and consequently tend to be larger and more broadly-spaced in the massive, more slowly cooled intrusive units (Plate 5.6A). Some of the finer-grained highly fractured massive units have slightly hummocky upper surfaces (Plate 5.6B) and these are most probably flows.

In the field the lighter colour of the low-Ti basaltic units is usually sufficient to distinguish them from Myra and Tamworth basaltic rocks. In addition, the low-Ti pillows display a far greater diversity of shapes and they lack the internal structures of the other types (compare Plates 3.1-3.4 with Plates 5.6 and 5.7). The associated hyaloclastites

PLATE 5.7

PBOC Hyaloclastite, Tomalla Creek Section (Map 1)

A. Tightly packed pillows partially surrounded by dispersed-framework hyaloclastite.

B. Pillow-fragment breccia. Pillow fragments are dispersed in a matrix of closed-framework hyaloclastite.

C,D. Discrete and budded lava tubes (largely in cross-section). Note relatively large phallic bud (*cf.* Ballard and Moore, 1977) in the centre and centre-right of C, and re-entrant structures in some 'pillows'. Interpillow hyaloclastite displays closed and slightly dispersed frameworks. Fields of view approximately 2 metres in width, *cf.* lens cap upper centre (C) and centre (D).

E. Composite enlargement of the central portion of the outcrop displayed in photograph D. Note elongate 'rafts' and smaller angular fragments of chloritized sideromelane (black) in the interpillow hyaloclastite. The white hyaloclastite matrix is largely chalcedony + carbonate. The elongate 'rafts' occurring to the left and upper right of the right lens cap clearly have spalled off the outer margins of the adjacent pillows.

F. Fragment of partially chloritized variolite (to the left of the lens cap) in closed-framework interpillow hyaloclastite. The margins of this fragment are delineated by a thin carbonate shroud. Individual varioles (spherulitically devitrified sideromelane, see text) display negligible alteration. This hyaloclastite was photographed through running water and most of the 'white veins' to the left and right of the variolite fragment are in fact reflections from the water surface.

G. Irregular 'V'-shaped fragment of aphanitic low-Ti basalt (dark grey, with lighter grey altered margins) in a specimen (040) of PBOC interpillow hyaloclastite. Angular black fragments are chloritized sideromelane. White - pale grey matrix is impure milky chalcedony.

PLATE 5·7

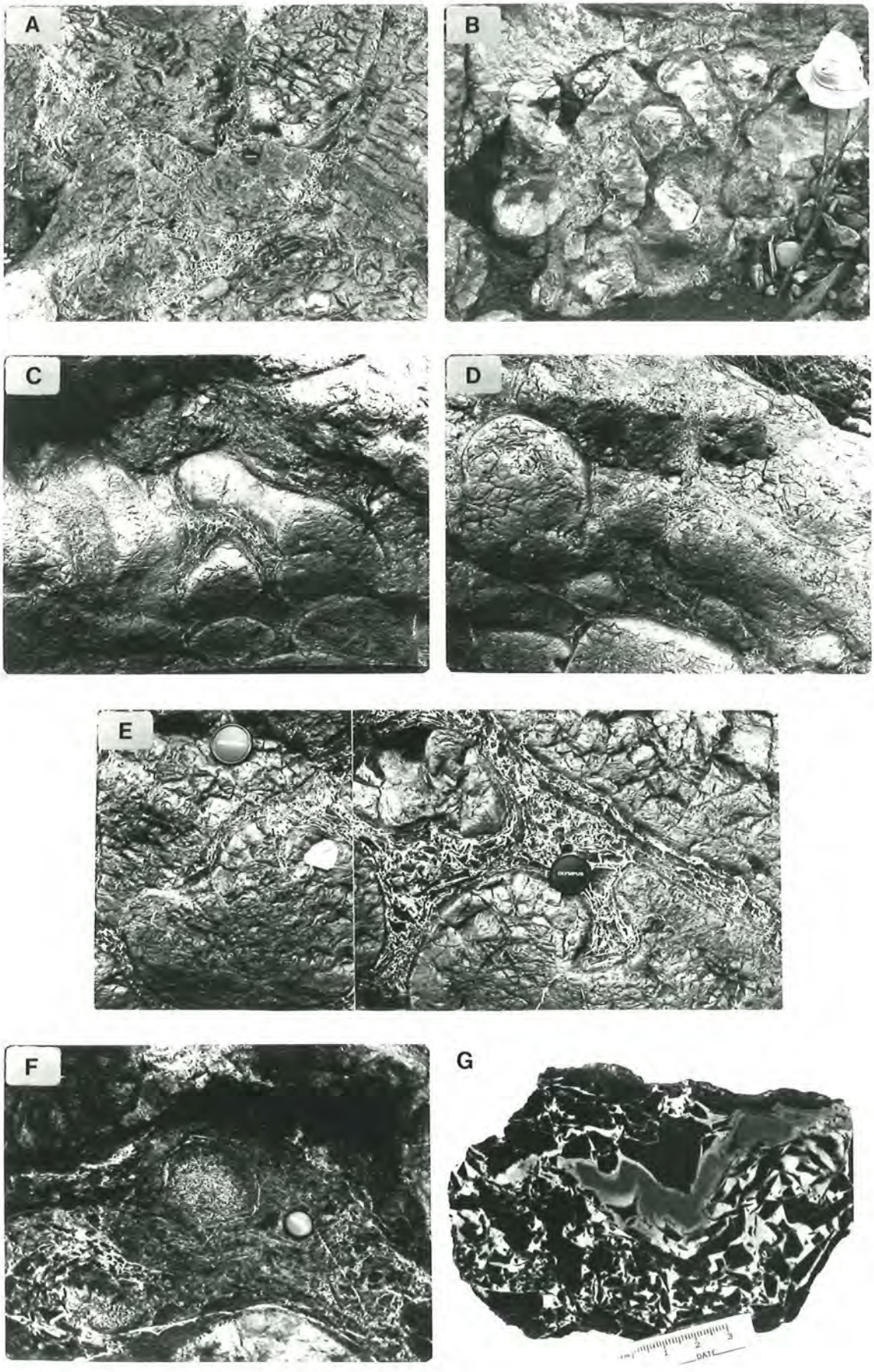

are also quite distinctive.

5.7.2 Petrography

(1) Primary Characteristics

With the exception of several microdoleritic intrusives (e.g. 005), low-Ti basaltic rocks from the PBOC are characterized by textures indicative of rapid to extremely rapid quenching (see discussion of quench textures in Section 3.3). Indeed, most of the microdoleritic types also contain a significant proportion of skeletal and spherulitic phases (e.g. 017, 023), and every gradation occurs between the quench textures in these rocks and the practically aphyric, spherulitically devitrified sideromelane in some of the pillowed extrusives.

To facilitate the description of textures in the low-Ti basaltic rocks they are divided into three textural types, termed variolites*, aphanites and microdolerites. The variolites predominantly consist of spherulitically devitrified sideromelane, the microdolerites are largely crystalline, and the aphanites are more-or-less transitional between variolites and microdolerites. It must be emphasized that these three textural types are convenient subdivisions of a continuum of textures formed in these rocks in response to differing degrees of crystallinity at the time of eruption, and to variable rates of cooling. However, on average the variolites do appear to be the more primitive types (see Section 5.7.4). Some pertinent petrographic characteristics of the hyaloclastites are described in part (2) of this section.

Primary mineral phases in the low-Ti basaltic rocks include essential plagioclase and Ca-rich pyroxene ± relatively minor amounts of olivine (invariably pseudomorphed) and Cr-Al spinel or rare Fe-Ti oxides. Trace amounts of (?) primary pyrite occur in some samples (e.g. 009).

Variolites

On a mesoscopic scale the low-Ti basaltic pillows are distinctively

---

* The term variolite is used here as a name for rocks consisting largely of varioles (spherulites in this case). This usage is similar to that of Gelinas *et al.* (1976) except that, for reasons unspecified, those authors restrict the term to rocks containing varioles set within a matrix.

aphyric and are often remarkably variolitic (abundant spherulites). In fact some pillows consist almost entirely of coalesced spherulites (Plate 5.8A). These spherulites may approach 1 cm in diameter in the interiors of the larger pillows and in general they gradually decrease in size towards the pillow margins where they may be microscopic. Most variolitic pillows have a chloritized outer rind which contains "free-floating" or clustered spherulites (Plate 5.8A,B) and fragments of this material are common in the interpillow hyaloclastites (Plate 5.7F,G).

Irrespective of their position within individual pillows these spherulites consist of surprisingly fresh (see Section 5.7.4) axially devitrified purplish-brown sideromelane with overlapping fine fibrous sheaf-like internal textures (Plate 5.8C,D). Beneath the outer chloritized zone they coalesce to form a polyhedral cell or "foam" texture (Plate 5.8A,B) with small blebs of secondary albite ± chalcedony (± carbonate) often occurring along the boundaries, and occasionally occupying triple-point junctions (Plate 5.8 C,D). Scattered discrete and clustered sheaf-like spherulitic aggregates of Ca-rich pyroxene ± plagioclase and highly acicular albitized plagioclase microlites occur within many of the devitrification spherulites, while others transgress spherulite boundaries (Plate 5.8 C,D). Some devitrification spherulites appear to have nucleated on these crystalline phases.

Pre-quench crystals are rare in the variolites. Plagioclase is the most abundant and most widespread microphenocryst phase. In most cases plagioclase microphenocrysts are pseudomorphed by albite ± chlorite ± carbonate ± prehnite assemblages but relict grains of anorthite (An_{92}, sample 002) do occur. Serpentine or chalcedony ± chlorite pseudomorphs (0.1 mm - 1.5 mm) after olivine euhedra (Plate 5.8E) or partially skeletal microphenocrysts (Plate 5.8F) are sparsely scattered throughout these variolitic types. On occasion these may contain small (<0.05 mm) red-brown spinel inclusions (Plate 5.8F) and similar spinels are also sparsely scattered throughout the spherulites in most samples (e.g. 003, 004). Pyroxene is confined to quench spherulitic intergrowths (commonly dendritic) with plagioclase, and Fe-Ti oxides do not occur in these rocks. Quench plagioclase is usually albitized.

Aphanites

These include examples from pillowed and massive cooling units and

PLATE 5.8

Textural Characteristics of PBOC Low-Ti Basaltic Rocks

A. Coalesced polygonal spherulites in a specimen (002) from near the margin of a variolitic low-Ti basalt pillow. Irregular white veins are carbonate and black inter-spherulite material near the left margin of the specimen is chlorite,presumably replacing sideromelane.

B. Coalesced and dispersed basaltic spherulites in a matrix of black chloritized (?)sideromelane. Note axial and radial devitrification structures in the spherulites. This specimen (039) is from the chloritized outer margin of a variolitic pillow.

C. Coalesced polygonal spherulites consisting of radially devitrified sideromelane. Note polygonal and subparallel cracking within spherulites. Dark fibrous patches are dendritic, axiolitic and sheaf-like spherulitic clinopyroxene. Highly acicular crystals (e.g. centre, and lower right corner) are albitized plagioclase. White inter-spherulite blebs are albite [sample 003, mag. = 22x, plane-polarized light].

D. Composite photomicrograph of fine fibrous radial, sheaf-like and subaxiolitic textures in spherulitically devitrified purplish-brown sideromelane. The core of the spherulite to the right of centre is occupied by a highly skeletal plagioclase microlite. The dark sub-rectangular patch near the lower margin approximately 2 cm from the lower left corner is an axiolitic clinopyroxene spherulite. Note the excellent preservation of extremely delicate devitrification textures [sample 003, mag. = 35x, crossed nicols].

E. Rare euhedral olivine microphenocryst now pseudomorphed by chalcedony (white) and chlorite (high relief). Irregularly-shaped black blebs within the microphenocryst are melt inclusions. Rounded and elongate black patches in the host devitrified sideromelane are clinopyroxene spherulites [sample 001, mag. = 20x, plane-polarized light].

F. Partially skeletal olivine microphenocrysts now pseudomorphed by carbonate. Black subequidimensional inclusions in both grains are Cr-Al spinels [sample 020, mag. = 90x, plane-polarized light].

G. Well-preserved sheaf spherulites of Ca-rich pyroxene in a pillowed low-Ti aphanitic extrusive [sample 011, mag. = 2x, crossed nicols].

H. Skeletal and acicular plagioclase in a groundmass of relatively coarsely crystalline 'open' spherulites of Ca-rich pyroxene in a massive aphanitic low-Ti basaltic cooling unit. Black grains included in plagioclase microphenocryst are in fact translucent red-brown Cr-Al spinel [sample 006, mag. = 35x, plane-polarized light].

PLATE 5·8

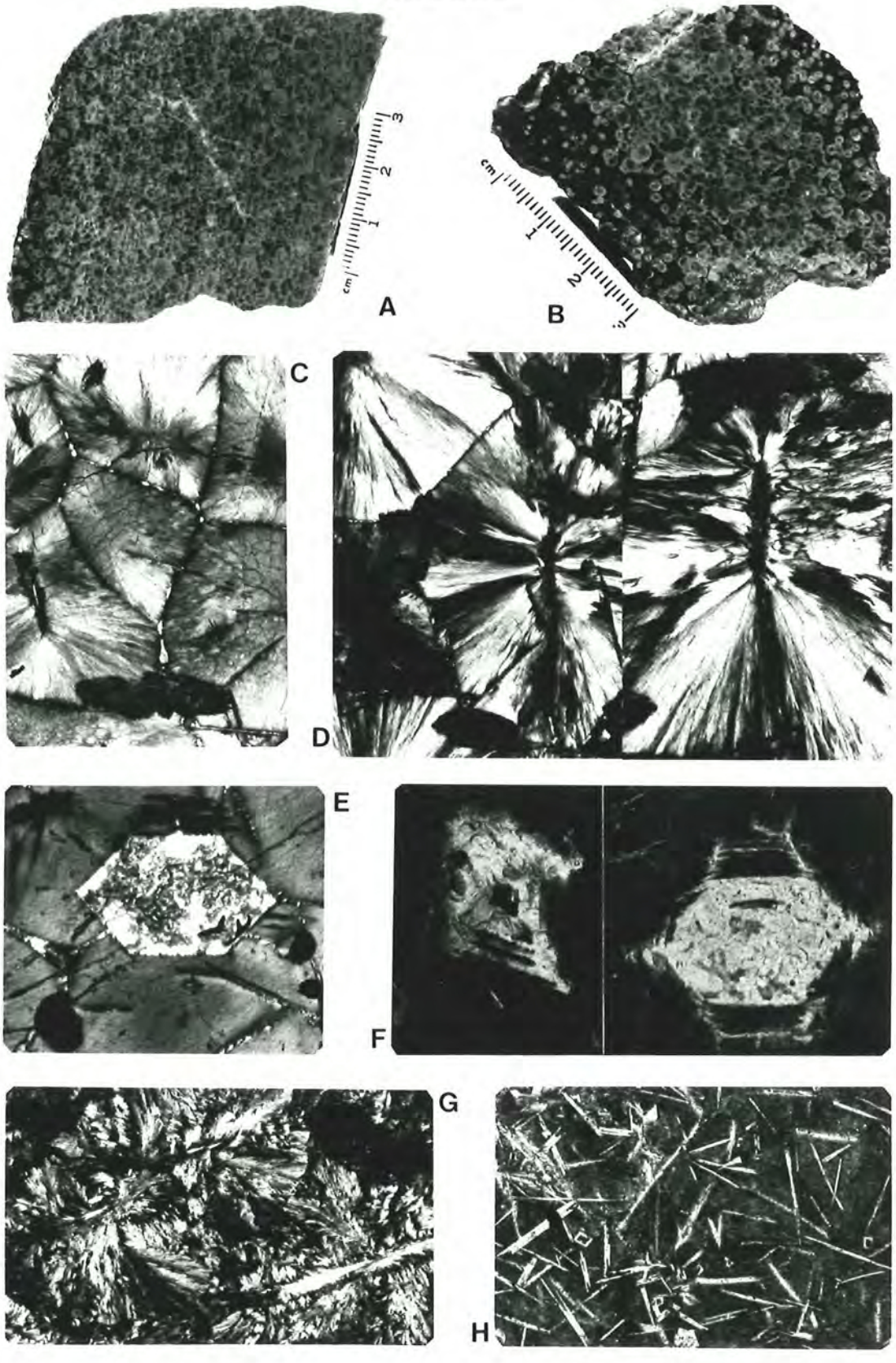

they constitute by far the most voluminous textural type. As might be expected from the rapid growth-rate of spherulitic pyroxene ± plagioclase in quenched basaltic melts (Schiffman and Lofgren, 1982), samples with textures intermediate between the quenched aphanites and the variolites (e.g. 010, 016) are relatively uncommon.

Within individual cooling units, including single pillows, the aphanites display a much greater degree of textural diversity than the variolites. The more rapidly quenched aphanites chiefly consist of spherulitic Ca-rich pyroxene ± plagioclase and abundant randomly-oriented acicular and skeletal plagioclase (Plate 5.8 G). In the less-rapidly quenched examples these fibrous spherulites are more open and more coarsely crystalline, and discrete plagioclase crystals are more prismatic (Plate 5.8 H). Ragged, highly elongate Ca-rich pyroxene microphenocrysts (Plate 5.9A,B)may also accompany the coarse spherulitic types, and as the former become more equant the textures begin to resemble those in the slightly coarser-grained microdoleritic rocks.

As in the variolites, pseudomorphed olivine and fresh and altered plagioclase are the principal phenocryst phases. These rarely exceed 1 mm in longest dimension and invariably constitute less than several percent of the mode. Rare red-brown spinels occur in the groundmass in many of the finer-grained samples but appear to be absent from the more slowly-cooled types. On the other hand groundmass Fe-Ti oxides are sparsely scattered throughout some of the more slowly cooled types (e.g. 018) but these are exceptionally rare in the quenched aphanites. Fe-Ti oxides are, however, conspicuous groundmass phases in the vesicular types (see Section 5.7.1) (e.g. 015, 022). Groundmass plagioclase is often albitized.

Microdolerites

Textures in the microdolerites are intersertal (e.g. 017), sub-ophitic (e.g. 005) or transitional between the two (e.g. 008). In the intersertal types framework crystals of Ca-rich pyroxene and plagioclase are typically elongate, have ragged outlines, and acicular quench over-growths are common (Plate 5.9C). The interstices contain chloritized glass, pyroxene±plagioclase spherulites, plagioclase sphèrulites and minute Fe-Ti oxides. Interstitial patches are relatively minute in the subophitic types and Ca-rich pyroxene and plagioclase are considerably more prismatic and

relatively equant. Fe-Ti oxide is an essential but very minor phase. As in the aphanites, Fe-Ti oxides are most conspicuous in the amygdaloidal types and these, incidentally, have intersertal textures (e.g. 023). No aluminous spinels or pseudomorphs after olivine have been recognized in any of the microdolerites examined.

Discussion

In general, the range of textures displayed by the PBOC low-Ti basaltic rocks is that which might be expected in an extrusive-intrusive pile where basaltic magmas crystallized at widely varying rates from temperatures approaching their respective liquidi (e.g. Schiffman and Lofgren, 1982). However the textures of the variolites are somewhat unusual. These rocks do contain occasional Ca-rich pyroxene-plagioclase quench spherulites similar to those which predominate in the more rapidly quenched aphanites, but by far the most prominent textural element in the variolites is almost certainly due to the subsolidus devitrification of sideromelane because:

(i) Apart from minor included quench crystalline phases, individual spherulites are chemically homogeneous and have chemical compositions similar to that of the bulk rock (see Section 3.5.7). This effectively excludes an origin *via* separation of the melt into immiscible liquid fractions prior to quenching (e.g. Furnes, 1973).

(ii) The following characteristics favour a devitrification origin for this texture in preference to spherulitic growth during quenching of the magma (e.g. Schiffman and Lofgren, 1982). The internal texture of individual spherulites resembles conical sheafs of extremely fine fibrous material stacked in a radial array. This material is usually difficult to resolve optically and under high power extinction is generally somewhat diffuse. Skeletal quench crystals and typical highly dendritic quench spherulites of Ca-rich pyroxene ± plagioclase (*cf.* Schiffman and Lofgren, 1982) are commonly included in the larger devitrification spherulites. Most important however, bulk-rock X-ray diffraction scans indicate a

paucity of crystalline phases which, incidentally, are almost entirely Ca-rich pyroxene and plagioclase (other peaks (?) not sufficiently resolvable).

On petrographic grounds alone almost all PBOC low-Ti basaltic rocks, and especially the variolites, are immediately distinguishable from other basaltic rocks in the Pigna Barney-Curricabark area (*cf.* Chapter 3). Distinctive primary petrographic and mineralogical characteristics of some or all of the low-Ti types are:

(i) Extraordinarily delicate devitrification and quench textures.
(ii) Modal Cr-Al spinel.
(iii) Conspicuous modal olivine (now invariably pseudomorphed).
(iv) Extreme scarcity of macroscopic phenocryst phases.
(v) An overall crystallization sequence of Cr-Al spinel ± olivine → Cr-Al spinel ± olivine ± plagioclase → olivine ± plagioclase → plagioclase + Ca-rich pyroxene (→ Fe-Ti oxide). Both olivine and plagioclase microphenocrysts may contain inclusions of Cr-Al spinel, and Fe-Ti oxide is generally absent (see above).
(vi) Scarcity or complete lack of modeal Fe-Ti oxide (titanomagnetite).

It is likely that the presence of significant modal Fe-Ti oxide in the amygdaloidal types reflects elevated fO_2 in these melts, possibly because of the dissociation of H_2O (e.g. Haggerty, 1978; Sato, 1978). On the other hand fO_2 would appear to have been unusually low in the non-amygdaloidal, Fe-Ti oxide-free types. However, during the latter stages of their crystallization some low-Ti microdolerites (e.g. 005) possessed sufficiently high Fe^{3+}/Fe^{2+} ratios to precipitate minor intergranular Fe-Ti oxide (titanomagnetite).

Even after a cursory petrographic examination, only rarely might amygdaloidal low-Ti types (e.g. 022) and occasional low-Ti subophitic microdolerites (e.g. 017) be confused with Myra or Glen Ward basaltic rocks. Nevertheless, these too are significantly impoverished in modal Fe-Ti oxides compared with the Myra and Glen Ward types.

On the basis of extensive petrographic investigations (this study,

numerous other studies, e.g. unpublished theses and reports at the University of New England and many thin sections prepared by myself from rocks collected from outside the present study areas) it would appear that low-Ti basaltic rocks of the type described here are exceedingly rare in the NEO, and are possibly confined to the PBOC. However, rare occurrences of other low-Ti petrographic types are known from the Woolomin Association in the Glenrock Station area. There, Offler (1982) found several outcrops of basaltic rocks possessing incompatible element-depleted chemistry similar to that of the PBOC types. However, the Glenrock Station examples, are significantly Ca-rich pyroxene phyric and Fe-Ti oxide-bearing (Offler, 1982). They are also distinctly more altered than the PBOC types.

Despite the fact that the PBOC and Glenrock low-Ti basaltic types occur in two intrinsically different geological settings (see Chapter 1), their chemical similarities might suggest that they have a common or similar mode of origin. Possible relations between these rocks are discussed in Chapter 7.

(2) Secondary Characteristics

Considering their age (see Chapter 1) and general mode of emplacement, most low-Ti basaltic rocks in the PBOC have experienced remarkably little secondary alteration. On the other hand basaltic fragments in the associated hyaloclastites are usually pervasively altered. The overall alteration patterns displayed by basaltic rocks in the PBOC do have implications for their bulk chemistry and post-eruptive history, and some pertinent petrographic observations are summarized below.

General Comments: All low-Ti basaltic outcrops are extensively veined. Vein assemblages include carbonate ± albite ± chalcedony ± prehnite ± chlorite ± pyrite ± rare zoisite (019). Olivine is invariably pseudomorphed by secondary phases which are typically carbonate, chalcedony or chalcedony ± chlorite ± carbonate. Plagioclase is kaolinized only in the amygdaloidal rocks and sericitization has not been observed in any sample. Where present, amygdales consist of similar assemblages ± hematite.

Variolites: Except in the outer margins of pillows, textural and mineralogical alteration of spherulitically devitrified sideromelane and Ca-rich pyroxene spherulites would appear to be neglible. These have also

experienced minimal chemical modification (see Sections 5.7.3 and 5.7.4). Extraordinarily delicate quench and devitrification textures have been preserved in great abundance. Nevertheless most plagioclase microlites have been albitized and secondary albite ± occasional chalcedony and/or carbonate occurs intermittently or continuously along some boundaries between adjacent devitrification spherulites. At pillow margins inter-spherulite glass is invariably chloritized but Ca-rich pyroxene and devitrification spherulites commonly remain unaltered. However, some of the latter have thin cryptocrystalline alteration rims and are patchily replaced by albite.

Aphanites: Plagioclase may or may not be albitized. Plagioclase micro-phenocrysts are often partially replaced or wholly pseudomorphed by chlorite and/or carbonate ± prehnite. Ca-rich pyroxene is almost invariably unaltered. Chlorite is abundant in the amygdaloidal rocks but in amygdale-free types it is confined to some olivine pseudomorphs and the outermost pillow rinds.

Microdolerites: Plagioclase is commonly fresh in the subophitic types and partially albitized in the intersertal types. Similarly, chlorite often replaces interstitial material, especially in the amygdaloidal examples, but is rare in the subophitic types (e.g. 005).

Hyaloclastites: With relatively few exceptions (e.g. Plate 5.6 F,G) basaltic fragments in the hyaloclastites are highly altered. Although these fragments and the intervening material display a considerable variety of complex secondary alteration textures and mineral assemblages, only those aspects of their general petrography pertinent to the post-eruptive history of the low-Ti basalt pile as a whole are reported here.

Most of the basaltic fragments are partially or completely replaced by large optically continuous masses of chlorite. These display relict perlitic cracks and concentric liesegang-like structures which resemble textures commonly seen in palagonitized sideromelane (*cf.* Dimroth and Lichtblau, 1979). In many such fragments the outer margins and zones along cross-cutting fractures consist of various combinations of: (i) bleb-like or botryoidal colourless- pale brown andradite (see Analysis 16, Table C-8), (ii) strongly pleochroic (deep green-colourless or pale yellow)

PLATE 5.9

A,B. Ragged elongate Ca-rich pyroxene microphenocrysts in PBOC aphanitic basaltic extrusives. These microphenocrysts appear to have been randomly oriented within flow-planes prior to final cooling. Note acicular and coarse spherulitic quench overgrowths of Ca-rich pyroxene, especially in B. In both (all) examples the groundmass entirely consists of quench clinopyroxene and plagioclase (commonly albitized) [samples 013 (A) and 007 (B), mag. = 35x, crossed nicols].

C. Intersertal/interstitial texture in PBOC low-Ti microdolerite. Relatively coarse-grained crystals are plagioclase and Ca-rich pyroxene. Note irregular quench overgrowths. Intersertal/interstitial dark grey mottled material is chlorite presumably replacing original glass or microlitic groundmass [sample 023, mag. = 35x, crossed nicols].

D. Altered sideromelane fragments in PBOC interpillow hyaloclastite. High relief white material at or near the margins of these fragments is colourless-pale brown andradite. Dark grey interiors and light grey cross-cutting veins are deep green and pale greenish-yellow chlorite respectively. The medium grey zone commonly developed between the andradite margins and the dark green chlorite cores consists of prehnite + minor cryptocrystalline chlorite. The matrix consists of chalcedony + prehnite + minor chlorite, carbonate and albite [sample 010(b), mag. = 22x, plane-polarized light].

E. Spherulitic and planar-fibrous pumpellyite (dark grey and light grey respectively) and (?) gel-palagonite (broad pale-medium grey zone displaying diffuse liesegang-like structures) lining fractures in a chloritized sideromelane fragment (chlorite lies adjacent to palagonite, note sharply defined contact) in PBOC interpillow hyaloclastite [sample 038, mag. = 35x, plane-polarized light].

F. Similar to E. Pumpellyite is relatively coarser-grained and is associated with minor albite + chlorite [sample 038, mag. = 22x, plane-polarized light].

PLATE 5·9

A

B

C

D

E

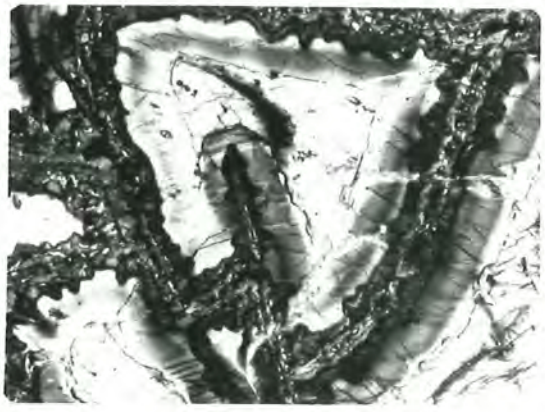

F

pumpellyite in spherulitic, acicular or planar-fibrous habit, and/or (iii) an amorphous pale brown to olive-brown clay-like material with extremely low birefringence (Plate 5.9 D,E,F). X-ray diffraction scans of the latter mineraloid did not produce any well-defined peaks. This material may well be a form of gel-palagonite (see Dimroth and Lichtblau, 1979). In many instances it is partially replaced by colloform bands or spherulitic patches of pumpellyite (Plate 5.9 E,F). The strong colour and pleochroism of the pumpellyite would suggest that it is an Fe-rich variety (Bishop, 1972; Kawachi, 1975; Trzcienski and Birkett, 1982). Other commonly abundant secondary phases in the basaltic fragments include prehnite, carbonate, albite and brown cryptocrystalline clay-like minerals. Microlitic fragments usually contain relatively fresh relict Ca-rich pyroxene (e.g. 037).

The hyaloclastite matrix largely consists of chalcedony. This is commonly ferruginous (jasper) in hyaloclastites associated with amygdaloidal pillows (Plate 5.6 H, sample 036). Pumpellyite, prehnite, carbonate, chlorite and clay minerals may be locally abundant (e.g. 010(b)), and trace amounts of sulphide may occur. Epidote is exceedingly rare.

Discussion

The wholesale preservation of extremely delicate spherulitic devitrification textures in the relatively unaltered sideromelane of the variolites, and the similarly delicate quench textures preserved in the aphanites, all strongly suggest that the PBOC low-Ti basaltic pile has not experienced burial metamorphic conditions of any consequence. In most of these basaltic rocks partial albitization of plagioclase constitutes the only significant secondary modification observed. Apart from very rare occurrences of prehnite partially replacing plagioclase microphenocrysts (e.g. 002) and chalcedony ± chlorite pseudomorphing olivine, burial metamorphic assemblages are rare, to say the least, in all but the amygdaloidal types. Pumpellyite, for instance, has not been found in any of the 47 thin sections of low-Ti basaltic rocks (including the amygdaloidal types) examined in this study.

At first sight secondary assemblages in the hyaloclastites would appear to be at variance with the above conclusions. In rocks of basaltic composition, prehnite + pumpellyite (± chlorite ± garnet)-bearing assemblages

are usually confined to moderately low-grade burial- or regional metamorphic terranes (e.g. Coombs *et al.*, 1970; Zen, 1974; Pluysnina and Ivanov, 1981; Houghton, 1982). Nevertheless, these phases can occur at low confining pressures in active geothermal areas (Sigvaldason, 1962) and on rare occasions in hydrothermally altered MORB and MORB breccias (Hekinian, 1973; Mevel, 1981) and their ophiolitic equivalents (e.g. Liou, 1979). In particular, Mevel (1981) describes prehnite- and pumpellyite-rich metabasalts from the Vema Fracture Zone (MAR) in some detail. She concludes that these secondary assemblages formed at temperatures of ~250°C and at very low confining pressure (<1 kb) during the hydrothermal circulation of seawater through their basaltic hosts. Growth of andradite-hydrogrossular garnet may be rapid at somewhat lower temperatures (~<170°C, Easton *et al.*, 1977,1982) in ocean-floor hydrothermal systems, and albitization of calcic plagioclase may readily occur at even lower temperatures (~110-120°C, Boles, 1982).

Clearly, it is quite feasible and indeed highly likely that the "prehnite-pumpellyite facies" assemblages in the PBOC hyaloclastites developed during relatively low temperature (<300°C) hydrothermal circulation through these highly permeable portions of the basaltic pile. Minimal alteration in the intimately associated glassy pillow lavas suggests that this hydrothermal activity was relatively short-lived, extremely localized and occurred at lithostatic pressures indicative of minimal overburden. In addition, in the hyaloclastites the replacement of sideromelane by chlorite ± pumpellyite rather than epidote suggests that little palagonitization took place prior to the development of these assemblages, and that the hydrothermal fluids were characterized by low fO_2 and μCO_2 (see Coombs *et al.*, 1970; Glassley, 1974; Baragar *et al.*, 1979; Liou, 1979). Considering the relatively rapid rate at which sideromelane may become palagonitized, even under very low temperature hydrothermal conditions (Furnes, 1975; Jakobsson, 1978), it is likely that much of the alteration of the PBOC hyaloclastites took place only a short time after their formation, possibly even during initial cooling of the associated lavas. Where palagonitization has occurred in these rocks, the palagonite(?) is only partially replaced by chlorite and pumpellyite, further suggesting that the hydrothermal event was short-lived and that for the most part, alteration occurred under reducing conditions. However, minor Fe-staining and the presence of jasper in the amygdaloidal rocks does indicate

some localized oxidative alteration.

Early deposition of fracture-filling albite ± chalcedony in the pillow lavas may have inhibited direct access of fluids to pillow interiors during hydrothermal events. This, combined with unusually reducing conditions, may have contributed significantly to the preservation of otherwise highly reactive components such as metastable quench pyroxenes and delicately devitrified sideromelane in the low-Ti basalt pile (*cf.* Furnes, 1975).

In the hyaloclastites, chalcedony and carbonate were probably deposited during the waning stages of hydrothermal activity when fluid circulation was becoming increasingly restricted (see Section 3.5.1(3)(i)). Elevated μ_{Si} at this stage could also explain the lack of zeolites in these rocks.

Petrographic evidence therefore, would strongly suggest that, unlike much of the adjacent Tamworth Belt succession, the PBOC low-Ti basaltic pile has not been significantly buried at any stage in its geological history. This supports field evidence for a substantial structural break between these adjacent lithologies (see Chapter 1). However, in the Glen Ward beds the occurrence of zeolite-rich hyaloclastites and practically unaltered quench-textured basaltic rocks amongst prehnite-pumpellyite facies volcaniclastics would suggest that significant structural breaks occur within these Tamworth Belt rocks too (see Chapters 1 and 3).

5.7.3 Mineral Chemistry

With the exception of Cr-Al spinels, groundmass mineral phases in most PBOC low-Ti basaltic extrusives almost invariably display crystal morphologies indicative of rapid metastable growth during quenching of the host melt (see Bryan, 1972; Lofgren, 1974; Fleet, 1975; Schiffman and Lofgren, 1982). In this study the chemistry of quench phases has not been examined in any detail. Rather, a large number of quench grains were analysed semiquantitatively by microprobe (counting time of 10 seconds) in an attempt to detect Ca-poor pyroxene and relict calcic plagioclase. Ca-poor pyroxene was not found but relict calcic plagioclase is relatively abundant in all but the more rapidly quenched types. Some representative analyses of groundmass pyroxenes and plagioclases are listed with analyses

of some less rapidly quenched examples in Tables E-1 and E-11, respectively. Analyses of groundmass Cr-Al spinels are listed in Table E-9. Acceptable quality analyses of Fe-Ti oxides are not available.

(1) Ca-rich Pyroxene

As might be expected from the general chemistry of their hosts (see Section 5.7.4), all Ca-rich pyroxenes in the low-Ti basaltic rocks are relatively enriched in SiO_2 and are strongly depleted in Na_2O and TiO_2. In fact, for most grains analysed TiO_2 levels were below the detection limit of the microprobe (0.07 wt %, see Appendix G). Those analyses listed with less than 0.07% TiO_2 (Table E-1) represent averages of several TiO_2 determinations, some of which are >0.07%.

Although Ca-rich pyroxenes with high SiO_2 and low TiO_2 are common in tholeiitic basalts, and in particular IAT (e.g. Nisbet and Pearce, 1977; Leterrier *et al.*, 1982), most PBOC pyroxenes contain considerably less TiO_2 than those from tholeiites in general. In fact they contain even less TiO_2 than Ca-rich pyroxenes in other highly incompatible element-depleted rocks such as basaltic and peridotitic komatiites (*cf.* Bickle *et al.*, 1975; Echeverria, 1980a; Dixon, 1981) and boninites (e.g. Kuroda *et al.*, 1978).*

Pyroxenes in the aphanitic rocks are all augites with *Ca* ranging from 31-39 and *mg* ranging from 55-78 (Fig.5.5, Table E-1, and unlisted analyses). The larger grains are commonly zoned to more Fe-rich compositions (e.g. 016) but the smaller spherulitic types are of fairly uniform compositions or else display only irregular zoning. However, considerable inter- and intra-grain variations in Al_2O_3 are common. The Al_2O_3 contents of most grains fall in the range 2%-4% (e.g. Table E-1) but grains with Al_2O_3 contents as low as 1.4% and as high as 5.7% have been found in these rocks. In some instances these analyses might reflect the presence of submicroscopic plagioclase intergrown with the spherulitic pyroxene, but for the most part the Al_2O_3 variations in these pyroxenes are likely to be the result of metastable crystallization during rapid cooling (see Section 3.3).

Pyroxenes in the low-Ti microdoleritic rocks are generally zoned

---

* Most Ca-rich pyroxenes in sample 015 (see Table E-1) contain <0.2% TiO_2. The analysis listed, however, is the only one from that sample which summed to an acceptable total (101%> <99%).

from diopsidic augite to augite (Table E-1). The diopsidic augite cores typically contain significant Cr_2O_3 (0.2%-0.9%) whereas the augite rims are depleted in Cr_2O_3 (<0.15%). On the other hand the pyroxene rims may contain detectable Na_2O (>0.1%) and commonly have lower *Ca* values than the cores. Zoning with respect to Al_2O_3 is often relatively slight and irregular but some rims contain up to 4.9% Al_2O_3. These Al-rich rims are presumably late-stage metastable growths. Calculated Fe^{3+} does not display regular zoning patterns and in any event these values are probably unreliable (see Section 3.3), especially in the quenched grains.

By far the most distinctive and distinguishing characteristic of Ca-rich pyroxenes in the low-Ti basaltic rocks is their exceptionally low TiO_2 contents. Even the Ca-rich pyroxenes in those samples which are largely devoid of modal Fe-Ti oxide (e.g. 009, 016) contain much less TiO_2 than their respective hosts (*cf.* Table 5.6a). This would suggest that an unrecognized cryptocrystalline(?) TiO_2-rich phase (possibly sphene) may be present. In all other aspects of their chemistry the Ca-rich pyroxenes in these rocks resemble those in saturated or slightly over-saturated tholeiitic basalts (*cf.* Deer *et al.*, 1978; Leterrier *et al.*, 1982), and in particular they resemble slightly less TiO_2-depleted Ca-rich pyroxenes in basaltic rocks from the Pindos and Troodos ophiolites (Capedri and Venturelli, 1979, analyses 8A,8B and 10). It is not known whether the TiO_2-depleted pyroxenes analysed by Capedri and Venturelli (1979) are from the boninite-like low-Ti basaltic extrusives in the Troodos (Simonian and Gass, 1978; Cameron *et al.*, 1979) and Pindos (Capedri *et al.*, 1980) ophiolites but this would seem likely.

(2) Plagioclase

In many of the low-Ti basaltic rocks groundmass plagioclase is largely albitized and plagioclase microphenocrysts are altered to albite ± carbonate ± chlorite ± prehnite assemblages. However, relicts of calcic plagioclase are relatively common in most samples, and predominate in samples 005, 006, 007 and 016 (Table E-11).

Scattered anorthite (An_{92-91}) microphenocrysts of essentially identical composition occur in samples 002 and 007. These coexist with groundmass bytownite (Table E-11) which is typically of fairly uniform composition. In these samples the groundmass plagioclases contain

considerably more Fe than the associated microphenocrysts (Table E-11). This is probably due to increased incorporation of Fe into the groundmass plagioclases during rapid cooling (Schiffman and Lofgren, 1982). The lack of co-precipitating Fe-Ti oxides in these rocks (presumably the result of low fO_2 in the melt, see Section 5.7.2) might have also contributed to enrichment of Fe in quench plagioclases.

The most sodic primary (?) plagioclase found in the low-Ti basaltic rocks is sodic andesine (An_{33}). Plagioclase in sample 015 is almost entirely albite ($An_{<3}$) and a single determination of An_{22} (Table E-1) is probably indicative of a partially albitized grain. In all plagioclases analysed, including secondary albite, K_2O is below the detection limit of the microprobe (<0.06%) and absence of sericitization is hardly surprising. Where analysed, MgO was also undetectable (<0.1%).

(3) Cr-Al Spinel

Cr-Al spinels in five samples from four low-Ti basaltic extrusives have been analysed by microprobe. These spinels are largely unzoned translucent tan to reddish-brown magnesiochromites (Table E-9), although some possess slightly more Fe-rich opaque outer rims. Single populations displaying limited chemical variation occur within each sample. Spinel populations in separate samples from a single pillow (001, 003), however, differ slightly in their chemistry (Table E-9, Fig. 5.3) and this would suggest that more extensive sampling of these rocks might reveal a somewhat broader range of spinel compositions than reported here. Low levels of SiO_2 (<0.2%) were found in a small percentage of analyses but replicate analyses of the same spots often failed to redetect SiO_2. Consequently all average analyses contain levels of SiO_2 well below the microprobe detection limit (<0.1%) and these values are not reported in Table E-9. In all spinels CaO abundances are below the microprobe detection limit (<0.07%).

All Cr-Al spinels in the PBOC low-Ti basaltic extrusives have M and Cr (100 Cr/(Cr+Al)) values and $Cr:Fe^{3+}:Al$ ratios within the ranges displayed by Cr-Al spinels in MORB (Figs 5.3c,d, 5.4). Compared with the remainder, those in samples 001 and 003 have slightly higher M values and Ti contents, and are markedly enriched in Al and depleted in Cr (Figs 5.3d, 5.4). Spinels in sample 003 have M values averaging 6-7% higher

than their host, but *M* values of spinels in the other samples are either equivalent to or slightly less than *M* values of their respective hosts (compare Tables 5.6a and E-9). Overall, spinels in the low-Ti basaltic rocks have higher *M* values than those in the majority of mafic and ultramafic intrusive members of the PBOC (Groups 1-4), and at a given *M* value the low-Ti basalt spinels also have higher *Cr* values and higher Fe^{3+}, V and Ti contents (Fig. 5.3). Nevertheless, their Cr-Al-Mg-Fe relations are well-within the overall range displayed by spinels from alpine peridotites (Figs 5.3c,d; 5.4).

During the crystallization of basaltic melts, Cr-Al spinel-melt compositional relations would appear to be significantly influenced by a complex interplay of physical and chemical factors. Thus crystallization of relatively aluminous spinel compositions may be favoured by elevated pressure (e.g. Green *et al.*, 1972; Dick and Bryan, 1978; Fisk and Bence, 1980) and/or an Al-and/or Mg-enriched melt (e.g. Sigurdsson and Schilling, 1976; Fisk and Bence, 1980) and/or late crystallization of plagioclase relative to spinel (Irvine in Dick and Bryan, 1978; Fisk and Bence, 1980) and/or low fO_2 (Fe^{3+} may substitute for Al^{3+} at elevated fO_2, Fisk and Bence, 1980). In addition, Fisk and Bence (1980) show that in spinels crystallizing from (?) primitive MORB (*M* = 68) at low pressure; (i) *Cr* initially decreases with decreasing temperature and then increases following the appearance of plagioclase on the liquidus (see also Irvine 1977b) and (ii) *M* spinel is commonly ~1.05 *M* liquid and this relationship is more-or-less maintained as *M* decreases with decreasing temperature (i.e. increasing olivine crystallization). Also, the Ti and Fe contents of spinels crystallizing from basaltic liquids tend to increase with decreasing temperature (increasing crystallization) (e.g. Misra and Taylor, 1977; Ridley, 1977; Eales *et al.* 1980).

Consequently, in view of the range of potential controls on spinel compositions during the early stages of basalt crystallization, it is not altogether surprising that spinel populations in many individual MORB, for example, display large compositional ranges (especially in *Cr*), even on the scale of a single thin section (e.g. Sigurdsson and Schilling, 1976; Dick and Bryan, 1978; Fisk and Bence, 1980; O'Donnell and Presnall, 1980). Fisk and Bence (1980) recognized three generations of spinels in FAMOUS basalt 527-1-1 (*M* = 68). In order of crystallization

these spinels are termed Group I (low *Cr*), Group II (high *Cr*) and Group III (intermediate *Cr*) (see Fig. 5.3d). Using 527-1-1 as starting material Fisk and Bence (1980) synthesized spinels similar to Groups II and III and they found that in liquids of this composition* Group II spinel is the low-pressure (1 atm.) liquidus phase and Group III spinel crystallizes at slightly higher fO_2 30°-50°C below the liquidus. Fisk and Bence (1980) were unable to synthesize Group I spinels from the 527-1-1 melt at low pressure. The implications of these experimental results for the petrogenetic significance of the PBOC low-Ti basalt spinels are somewhat enigmatic.

The more aluminous (low *Cr*) low-Ti basalt spinels (in samples 001, 003) have *M* and *Cr* values and Al_2O_3 contents similar to Group III spinels in 527-1-1 (Figs 5.3d,5.12). The Group III and the Al-rich PBOC spinels also have comparable (calculated) Fe_2O_3 contents (~4.5%-5.0%). On the other hand, the relatively Al-poor low-Ti basalt spinels have appreciably higher *Cr* values than Group II and Group III spinels. In fact, the *Cr* values of these PBOC spinels approach the highest *Cr* values recorded for MORB spinels (Fig. 5.3d).

In contrast with 527-1-1 and numerous other MORB, however, high and low *Cr* spinels do not coexist in the PBOC low-Ti basaltic rocks. Nor do spinel Al_2O_3 contents reflect variations in host rock Al_2O_3 (Fig. 5.12). In fact within each group of low-Ti basalt spinels there is a slight antipathetic relationship between spinel Al_2O_3 and host rock Al_2O_3 (Fig. 5.12). In the high *Cr* spinels this slight trend of decreasing Al_2O_3 with increasing Al_2O_3 in their respective hosts also correlates with increasing modal plagioclase in the host, and as a group these rocks are noticeably plagioclase-phyric (and possibly slightly Cr-rich, see Table 5.6a) compared with the practically aphyric types (variolites) bearing the low-Cr spinels.

Thus, in the absence of textural data to the contrary, it is

---

* Anhydrous, 527-1-1 contains slightly more Al_2O_3 (~16.8%), considerably more TiO_2 (0.66%) and slightly less SiO_2 (~49%) than the more magnesian spinel-bearing PBOC low-Ti, basaltic rocks (analyses 1 and 3, Table 3.6a). In other aspects of their chemistry, including Cr contents, these rocks are quite similar (*cf.* Table 1 of Fisk and Bence, 1980).

possible that for samples 002, 004 and 006, spinel, olivine and plagioclase appeared on the liquidus almost simultaneously (anorthite microphenocrysts do occur in these rocks) and that the spinel was enriched in Cr as a result of competition for Al from plagioclase. The lower *Cr* values of spinels in samples 001, 003 would suggest that, in accord with petrographic indications, these may have crystallized slightly earlier than plagioclase. It is also possible that fO_2 was lower in these melts thus somewhat reducing the activity of Cr^{3+} (Hill and Roeder, 1974).

From the data available, however, one possibility that cannot be entirely overlooked is that Cr (and Ni) abundances were significantly greater in the pristine low-Ti basaltic melts (see Section 5.7.4), and that some removal of near-liquidus spinel ± olivine occurred prior to eruption. Thus the remaining high *Cr* spinels might not be entirely in equilibrium (w.r.t. Cr) with their hosts. The low-*Cr* spinels in the variolites also might have crystallized under similar circumstances, but at higher pressure and/or lower fO_2. Nevertheless, the surprisingly high Ti in some of these spinels relative to those in the other low-Ti basalts and those in 527-1-1 (including Group III) is difficult to explain in terms of an early crystallization model.

Clearly, details of the crystallization histories of spinels in the low-Ti basaltic rocks remain somewhat conjectural. On the other hand, an important empirical finding of this study is that, despite some similarities in whole-rock incompatible element chemistry between the PBOC low-Ti basalts and boninites (see Section 5.7.4), spinels in the low-Ti basalts far more closely resemble those in primitive MORB (Fig. 5.3d). This is consistent with the otherwise normal (except in TiO_2 and P_2O_5 abundances) major element chemistry of these PBOC extrusives (see below).

5.7.4 Whole-Rock Chemistry

Major and trace element analyses of PBOC low-Ti basaltic rocks are listed in Table 5.6a. These include three averaged broad-beam microprobe analyses of spherulitically devitrified sideromelane (analyses 2,3,6). Microprobe analyses 2 and 3 are from the same pillows as bulk analyses 1 and 4 respectively. With the exception of some anomalous minor element determinations (e.g. Ti, P, Mn, K) in analysis 2, and perhaps minor secondary modification of alkali abundances in all samples, the "sideromelane" - and bulk chemistries of samples 001-004 are sufficiently similar to suggest that

the bulk chemistries of the PBOC variolites (at least) approximate liquid compositions. Anomalously high V and Cr abundances in analysis 6 (see NOTE, Table 5.6a) reflect excessively high abundances of these elements (e.g. 0.35% Cr_2O_3, 0.31% V_2O_3) in two of the "sideromelane" varioles analysed (? sub-microscopic oxides). The remainder of the individual microprobe analyses contained "normal" V and Cr abundances similar to those in analysis 3.

Most of the samples selected for analysis contained some fine carbonate veins. Veined fragments were removed during initial crushing. Comparison of the chemistry of vein-rich fragments removed from sample 011 and equivalent vein-free material (Table 5.6a, analyses 15 and 11 respectively) suggests that, for this sample at least: (i) the Fe_2O_3/FeO ratio has not been significantly affected by veining [*cf.* Section 3.5.1 (3)]; (ii) except for a slight increase in Ca, the presence of any undetected veins in the "vein-free" samples analysed is unlikely to cause significant discrepancies in their observed chemistries, and (iii) Fe and Mg were not differentially mobilized during veining [Fe/Mg in 011 and 011(a) = 0.65 and 0.66 respectively].

Bulk chemical analyses of two interpillow hyaloclastites

010(a): predominantly (80-90%) chloritized sideromelane fragments + carbonate cement,

010(b): chloritized sideromelane fragments dispersed in a chalcedony-rich (+ carbonate) matrix,

suggest that extreme alteration of the low-Ti 'glassy' extrusives might conceivably lead to some leaching of Mn, Sr, Na and perhaps K, Ti and Y, and the introduction of some Ca, Li and P. Nevertheless, allowing for dilution by the carbonate cement in sample 010(a) and possible depletion in Ca and enrichment in Na during albitization of plagioclase in sample 010, the gross similarities in chemistry displayed by these two samples suggest that the abundances of most elements in samples displaying little petrographic evidence of alteration are probably very similar to those of the pristine basalt. In the aphanites and microdolerites, however, albitization of plagioclase has almost certainly led to some mobilization of Na and Ca. These elements might have been significantly less mobile in the variolites where plagioclase (albitized) is relatively rare.

Major and Minor Element Characteristics

Perhaps the most striking characteristic of the PBOC basaltic extrusives is their typically extreme depletion in K (commonly <0.1%) and the

TABLE 5.6a

Major and Trace Element Analyses of Low-Ti Basaltic Rocks from the Pigna Barney Ophiolitic Complex

ANALYSIS No.	1	2	3	4	5	6	7	8	9	10	11	12	13	14	+ Veins 15	Hyaloclastites 16	17
SAMPLE	001	002	003	004	005	006	007	008	009	010	011	012	013	014	011(a)	010(a)	010(b)
SiO_2	50.22	51.20	51.10	52.23	52.73	51.17	51.17	51.33	52.39	52.94	53.48	53.08	52.94	50.45	52.43	50.85	73.95
TiO_2	0.18	0.09	0.13	0.13	0.20	0.15	0.22	0.17	0.18	0.23	0.23	0.23	0.23	0.21	0.22	0.17	0.03
Al_2O_3	15.52	15.16	15.02	15.48	14.70	16.04	15.32	15.54	15.15	14.62	13.81	14.81	13.92	14.41	14.10	15.53	5.77
Fe_2O_3	0.94	0.92	0.98	0.90	1.01	1.04	1.10	1.09	1.13	1.10	1.11	1.16	1.24	1.16	1.19	3.94	3.37
FeO	7.60	7.51	7.90	7.32	8.16	8.43	8.92	8.80	9.13	8.91	9.02	9.44	10.01	9.41	8.84	6.74	2.74
MnO	0.16	0.05	0.13	0.18	0.18	0.20	0.21	0.21	0.23	0.20	0.20	0.20	0.21	0.21	0.20	0.11	0.05
MgO	10.31	9.90	9.78	9.00	9.27	9.49	9.57	9.42	9.54	8.95	8.68	7.99	8.28	7.54	8.39	8.10	2.82
CaO	12.35	12.55	13.01	12.21	11.02	10.36	11.71	10.43	10.13	9.08	9.13	9.74	8.77	13.85	11.21	14.19	10.97
Na_2O	2.34	2.62	1.79	1.86	2.21	2.76	1.77	2.69	2.30	3.33	3.74	2.96	3.67	2.41	3.77	0.36	0.22
K_2O	0.29	-	0.05	0.05	0.25	0.09	0.08	0.17	0.08	0.04	0.05	0.36	0.07	0.02	0.05	0.01	-
P_2O_5	0.03	-	0.03	0.04	0.04	-	0.04	0.04	0.04	0.03	0.04	0.05	0.04	0.04	0.04	0.03	0.12
TOTAL	99.94	100.00	99.92	99.40	99.77	99.73	100.11	99.89	100.30	99.43	99.49	100.02	99.38	99.72	100.54	100.03	100.04
ΣVol.[1]	4.10	1.39	0.69	1.46	2.93	2.09	2.88	3.60	3.80	2.73	1.75	2.68	3.52	3.40	2.72*	8.54*	6.70*
Fe_2O_3/FeO[1]	0.16			0.22	0.16		0.16	0.15	0.23	0.15	0.16	0.23	0.16	0.24	0.13	0.58	1.23
%	70.7	70.1	68.8	68.7	66.9	66.7	65.6	65.6	65.1	64.2	63.2	60.1	59.6	58.5			
TRACE ELEMENTS (μg/g)																	
K	-	n.d.	n.d.	433	-	n.d.	-	1460	698	324	404	-	554	136	n.d.	125	-
Rb	2			3	5		<2	3	3	<2	<2	7	<2	2		<2	<2
Ba	21			19	28		21	29	26	18	17	45	23	8		18	11
Sr	60			90	55		40	110	69	93	60	97	67	16		18	<1
Li				3.4	4.3			3.4	3.4	4.5	4.5	1.7	3.4	7.5		7.9	35
Zr	7			6	10		9	8	6	8	9	10	8	n.d.		7	2
Nb	3			<3	3		3	<3	<3	<3	3	5	<3	n.d.		<3	3
Y	11			9	18		15	12	14	18	18	15	17	16		12	12
Ti	988			909	1339		1316	1202	1276	1569	1555	1480	1565	1500		1362	n.d.
Cu	68			67	94		98	85	99	108	107	77	119	104		91	35
Zn	68			64	72		93	85	88	82	81	53	90	83		32	-
Ni	148			125	94		142	139	134	101	100	111	105	81		95	33
Co	78			85	73		71	70	<82	<65	<81	43	<82	74		60	30
V	242			226	274		328	300	322	323	318	341	352	332		282	123
Cr	430			535	345		282	428	356	265	256	281	155	144		n.d.	n.d.
La	<2			<2	4		3	2	3	5	5	3	4	n.d.		6	n.d.
Ce	6			9	7		8	7	9	9	10	9	9	n.d.		10	n.d.
Nd	<2			3	3		2	2	2	3	3	2	3	n.d.		2	n.d.
Sc	n.d.			51	63		n.d.	56	58	n.d.	n.d.	n.d.	n.d.	62		n.d.	n.d.

[1] See Appendix G.

% = 100 $Mg/Mg+Fe^{2+}$

n.d. = not determined.

* ΣVol includes significant CO_2

NOTE: Analysis 3 includes 0.05% V_2O_3 and 0.03% Cr_2O_3; Analysis 6 includes 0.12% V_2O_3 and 0.15% Cr_2O_3. Analyses 2,3 and 6 are each averages of 5 microprobe determinations from scans across spherulitically devitrified sideromelane. Sample 012 is from an amphibolitized basaltic dyke intruding low-Ti gabbros. Sample 011(a) contains abundant fine carbonate veins and is from the same cooling unit as sample 011. Samples 010(a) and 010(b) are inter-pillow hyaloclastite from the same outcrop as sample 010. Analyses 5,6,8 and 14 are of samples from massive cooling units (some possibly sills); analyses 1,2,3,4,7,9,10,11 and 13 are of samples from pillowed units.
Major element analyses are recalculated to original totals on a volatile-free basis; microprobe analyses are recalculated to 100% and volatiles determined by difference.
Trace element values are also recalculated on a volatile-free basis.

TABLE 5.6b

C.I.P.W. Normative Mineralogy of Low-Ti Basaltic Rocks from the Pigna Barney Ophiolitic Complex

ANALYSIS No.	1	2	3	4	5	6	7	8	9	10	11	12	13	14
SAMPLE	001	002	003	004	005	006	007	008	009	010	011	012	013	014
qz	-	-	-	1.67	0.56	-	-	-	-	-	-	-	-	-
or	1.71	-	0.30	0.30	1.48	0.53	0.47	1.00	0.47	0.24	0.30	2.13	0.41	0.12
ab	19.80	22.17	15.15	15.74	18.70	23.35	14.98	22.76	19.46	28.18	31.65	25.05	31.05	20.39
an	30.99	29.61	32.80	33.74	29.45	31.11	33.62	29.83	30.78	24.83	20.75	26.06	21.30	28.44
di	24.37	26.47	25.62	21.59	20.32	16.53	19.75	17.67	15.69	16.37	19.88	18.03	18.05	32.94
hy	6.15	8.26	20.86	24.70	27.32	16.05	27.84	17.06	31.24	22.33	17.40	24.16	18.36	6.65
ol	15.13	11.99	3.44	-	-	10.29	1.35	9.57	0.59	5.39	7.38	2.36	7.87	8.99
mt	1.36	1.33	1.42	1.30	1.46	1.51	1.59	1.58	1.64	1.59	1.61	1.68	1.80	1.68
chr	0.09	-	0.04	0.12	0.06	0.22	0.06	0.09	0.07	0.06	0.06	0.06	0.03	0.03
il	0.34	0.17	0.25	0.25	0.38	0.28	0.42	0.32	0.34	0.44	0.44	0.44	0.44	0.40
ap	0.07	-	0.03	0.09	0.09	-	0.09	0.09	0.09	0.07	0.09	0.12	0.09	0.09
Σ	100.01	100.00	99.91	99.50	99.82	99.87	100.17	99.97	100.37	99.50	99.56	100.09	99.40	99.73
100 an/(ab+an)	61.0	57.2	68.4	68.2	61.2	57.1	69.2	56.7	61.3	46.8	39.6	51.0	40.7	58.2

$Fe^{3+}/\Sigma Fe = 0.1$

relatively incompatible minor elements Ti (TiO_2 < 0.25%) and P (P_2O_5 ≤ 0.05%). In fact, they commonly contain less TiO_2 and have Al_2O_3/TiO_2, MgO/TiO_2 and CaO/TiO_2 ratios* lower than, or analogous to, the majority of relatively Ti-poor basaltic types (Fig. 5.13A,B; *cf.* Sun and Nesbitt, 1978; Hickey and Frey, 1982). However, in most aspects of their major element chemistry they closely resemble fairly typical tholeiites (e.g. Figs 5.13C,D; 6.1C; Table 5.6a). Thus, although they display a broad range of C.I.P.W. normative compositions (Figs 5.2, 5.14A; Table 5.6b), all contain significant *hy* (31%-6%) and most contain *ol* (<15%) or, on occasion, minor *qz* (<2%).

Compared with the most depleted MORB and many examples of depleted Ti-poor basaltic types** (e.g. boninites, high-Mg andesites, ophiolitic low-Ti basalts, basaltic komatiites; *cf.* references listed for Fig. 5.13, Tatsumi and Ishizaka, 1981, 1982a,b; Hickey and Frey, 1982) the PBOC low-Ti basalts are significantly depleted in the relatively immobile incompatible elements (e.g. Ti, P, and especially Zr), although they contain somewhat similar (low) abundances of the large-ion lithophile (LIL) elements (e.g. Ba and, on occasion, Rb and/or Sr) and, to a lesser extent, LREE (La + Ce + Nd < 15 µg/g for M > 65; for many boninitic types La + Ce + Nd < 5-20, e.g. Hickey and Frey, 1982). On the other hand, they typically contain significantly less Ni (150-80 µg/g) and Cr (540-140 µg/g), and significantly more V (220-350µg/g) and Sc (50-63 µg/g) than non-cumulate N-type MORB with comparable M values (71-58; *cf.* Basaltic Volcanism Study Project, 1981), and their Y contents are intermediate between boninites (<10 µg/g) and primitive MORB (20-30 µg/g). Needless to say, they are depleted in Ni and Cr, and enriched in V (Fig. 6.1j) and Sc relative to the majority of boninites and other Ti-poor basaltic rocks (in general, Ni > 150 µg/g, Cr 200-3000µg/g, V < 200 µg/g, and Sc < 40 µg/g; *cf.* Simonian and Gass, 1978; Dietrich *et al.* 1978; Coish and Church, 1979; Jenner, 1981; Hickey and Frey, 1982).

Other distinctive and/or somewhat anomalous trace element characteristics of the PBOC low-Ti basalts include: (i) exceedingly, and perhaps uniquely low Zr/Y (0.4-0.7; see Figs 5.16, 6.1a) and Zr/Nb (2-?4) ratios compared with other subalkaline basaltic rocks (e.g. Zr/Y in MORB > 1.5,

---

* Following slight alteration, Al_2O_3/TiO_2 and CaO/TiO_2 ratios currently displayed by some PBOC low-Ti basalts are probably slightly lower than pristine values (see later discussion).

** i.e., all basaltic-picritic rocks and high-Mg andesites containing less TiO_2 than the most depleted MORB (i.e. < 0.5% TiO_2). The terminology 'low-Ti basalts' as used here is restricted to Ti-poor basalts (i.e. SiO_2 ≤~53%, M ≤ 70).

IAT > 1.3*,Ti-poor basaltic rocks usually ≫ 2; Zr/Nb in MORB ≫ 4, IAT ≫ 10, Ti-poor basaltic rocks > ?20; see Basaltic Volcanism Study Project, 1981; Erlank and Kable, 1976; Flower *et al.*, 1977; Kay and Hubbard, 1978; Tarney *et al.*, 1978; Nesbit *et al.*, 1979; Pearce and Norry, 1979; Sun *et al.*, 1979; Jenner, 1981; Hickey and Frey, 1982 and references listed for Fig. 5.13); (ii) Ti/Zr ratios (120-180) intermediate between MORB (80-150) and Ti-poor basaltic rocks (100-600) see references listed above; (iii) relatively low Ni/Co ratios (1.1-2.6) intermediate between MORB (>1.5, usually falling in the range 2.5-7, e.g. Lambert and Holland, 1977; Langmuir *et al.*, 1977; Kay and Hubbard, 1978; Sun *et al.*, 1979; le Roex *et al.*, 1981) and IAT (Ni/Co < 1; Perfit *et al.*, 1979, 1980; Basaltic Volcanism Study Project, 1981), and significantly lower than most Ti-poor basaltic rocks (Ni/Co > 3?, e.g. Dietrich *et al.*, 1978; Hickey and Haskin, 1982); (iv) Cu (60-120 μg/g) and Zn (50-100 μg/g) abundances analogous to, and commonly greater than, those in N-type MORB (e.g. Flower *et al.*, 1977; Langmuir *et al.*, 1977; Kay and Hubbard, 1978; Tarney *et al.*, 1978; Basaltic Volcanism Study Project, 1981; le Roex *et al.*, 1981); and (v) anomalously high initial $^{87}Sr/^{86}Sr$ ratios (∿ 0.705), at least in the more crystalline types (see Appendix H, Table H-2), relative to fresh MORB ($^{87}Sr/^{86}Sr \leq 0.703$; relatively few strontium isotopic data are available for Ti-poor basaltic rocks, see Section 5.8).

Discussion

The more-or-less basaltic $100an/(ab + an)$ ratios (70-40, Table 5.6b) in most PBOC low-Ti basaltic rocks would suggest that the widespread albitization of plagioclase (see Section 5.7.3) might have only slightly or moderately affected Na and Ca abundances and, indirectly, *di*. However: (i) relict plagioclase in some of these low-Ti basalts is significantly more calcic ($>An_{70}$) than most of the normative plagioclase compositions; (ii) as a group the low-Ti basalts display gross trends of decreasing Al_2O_3 (? several sub-trends) and CaO with increasing *M* (Fig. 5.15) and these trends are inconsistent with the observed trends of increasing modal plagioclase + clinopyroxene with increasing *M*. That is, the decreases in Al and Ca are unlikely to reflect (1) plagioclase ± clinopyroxene fractionation (*cf.* trends of increasing Al_2O_3/MgO ratio with increasing TiO_2 displayed by MORB; Fig. 5.13A); or (2) successive/progressive partial melting of a refractory mantle source (see below) which should produce liquids displaying trends of decreasing Al_2O_3 and, ultimately, decreasing CaO with increasing *M* (e.g.

*At least one unusual Ti-poor (K,Rb,Ba,P,LREE - rich) basalt whose Zr/Y ratio is slightly <1 occurs in the Kurile-Kamchatka island arc (Popolitov and Volynets, 1982).

Duncan and Green, 1980; Jaques and Green, 1980; *cf.* Ti-poor basaltic rocks, fields 6-9, Fig. 5.13A).

Consequently, because secondary Al-bearing phases other than albite are rare in these rocks, and although Al is generally considered to be immobile [see Section 3.5.1(3)], it appears likely that some Al may have been lost during the albitization of Ca-rich plagioclase in the aphanites and microdolerites. Although losses of Al from these rocks may have reduced (*ab* + *an*) and increased *di*, concomitant loss of Ca would partly compensate for the latter without greatly affecting other normative relations (e.g. DI:OL:SILICA , Fig. 5.14B). Therefore, despite the constraints imposed by alteration, some tentative inferences on crystallization behaviour may be drawn from the C.I.P.W. norms of these rocks.

Although the (*ab* + *an*):*ol*:*di* relations in most of these PBOC basaltic rocks are similar to those displayed by relatively "primitive" TiO_2-poor (0.5%-0.9% TiO_2) MORB possessing comparable MgO contents (Fig. 5.14A), unlike MORB in general, many of the PBOC basaltic rocks plot within the orthopyroxene phase volume in the system DI:OL:SILICA for pressures in the vicinity of 5-10 kb (Fig. 5.14B, *cf.* Stolper, 1980). They do, however, cluster along the general trend displayed by MORB glasses in the PL:SILICA:OL projection (see Fig. 5.14C) of Walker *et al.* (1979) and Stolper (1980).

Therefore, although most PBOC low-Ti basalts are slightly enriched in SiO_2 (50%-53.5% SiO_2, Table 5.6a) relative to MORB with comparable MgO contents, their bulk chemistry is nevertheless consistent with the observed low-pressure, largely quench assemblages consisting of olivine + plagioclase + clinopyroxene, but apparently devoid of orthopyroxene (Fig. 5.14B,C; see Section 5.7.2). Figure 5.14B suggests that orthopyroxene would have been a potential phase crystallizing from the most *hy*-rich PBOC basaltic melts (e.g. Tables 5.6a,b, analysis 9) at pressures approaching 10 kb, and perhaps at significantly lower pressures. Although this implies that melts similar in chemistry to some of the PBOC basaltic extrusives were probably capable of yielding orthopyroxene-bearing cumulates superficially similar to some of the PBOC intrusives (e.g. the gabbros and olivine norites, Sections 5.4 and 5.5), possible genetic relationships between these extrusives and intrusives are ambiguous.

For instance, orthopyroxene precipitation from melts of PBOC low-Ti basalt composition ideally would have been facilitated if they had been sig-

nificantly hydrous, with consequent depression of their liquidi. However, most of the melts yielding the PBOC low-Ti basalts appear to have been relatively "dry" because they possess: (i) relatively low bulk Fe_2O_3/FeO ratios (commonly <0.2, Table 5.6a) despite some presumably oxidative alteration; (ii) clinopyroxenes with low (calculated) Fe^{3+} (e.g. Table E-1); (iii) highly calcic early-crystallized plagioclases (e.g. An_{92-91}, see Section 5.7.3; *cf.* Hamilton *et al.*, 1964; Kushiro, 1979); and (iv) they are devoid of primary hydrous phases and, with rare exceptions*, completely devoid of Fe-Ti oxides (see Sections 5.7.2, 5.7.3). These characteristics suggest that most of these melts contained significantly less H_2O than many relatively "dry" tholeiitic melts such as MORB (generally <0.3 wt % H_2O, see Section 3.6.1) which nevertheless contain sufficient "free" O_2 (presumably derived from the dissociation of H_2O) to crystallize relatively abundant late-stage titanomagnetite.

Although the PBOC intrusives also appear to have crystallized from essentially anhydrous melts [with very rare exceptions, see Section 5.3.1(iii); *cf.* PBOC olivine norites, for example, p. 216], the melts yielding these cumulates are unlikely to have been parental to (*via* cumulate formation) or analogous to those now represented by the PBOC low-Ti basalts because:

1. Early-precipitated orthopyroxenes ($mg \leq 79$) in the gabbros are even more Fe-rich than those which might be expected to be in equilibrium with the most Fe-rich low-Ti basalt ($M \sim 58$; *cf.* Section 5.5.4; see below).
2. The $\Sigma FeO:\Sigma FeO/MgO$ and Fe + Ti:Mg:Al relations ('Fe-enrichment trends', Figs 5.10 and 5.13D respectively) displayed by the PBOC gabbros, olivine norites and cumulate peridotites suggest that most of these intrusives are unlikely to be daughter cumulates which might have generated the Fe-enrichment trend in the low-Ti basalts by fractionation. Furthermore, the olivine norites most closely associated with the low-Ti basalts in the field (locality 3) display regular variations in chemistry which reflect the M values of their parental melts (derived *via* olivine compositions, see Section 5.4.4, Fig. 5.9). In the context of parent-daughter relations, Figure 5.15 clearly indicates that these chemical variations in the olivine norites are inconsistent with at least the Al, Fe, Mg, Ca, Cr and Ni variations with decreasing M in the low-Ti basaltic rocks.

---

* Some microdolerites contain a trace of titanomagnetite, as do the volumetrically insignificant amygdaloidal (?) low-Ti basalts (see Section 5.7.2). Compared with other PBOC basaltic rocks the amygdaloidal variants are highly altered. Consequently, they were not analysed and their probable "low-Ti" character remains unconfirmed.